Bacterial nucleoid dynamics: oxidative stress response in Staphylococcus aureus

doi: 10.1111/j.1365-2443.2006.00949.x

Bacterial Nucleoid Dynamics: Oxidative Stress Response in *Staphylococcus aureus*

Kazuya Morikawa[1,*], Ryosuke L. Ohniwa[2], Joongbaek Kim[2], Atsushi Maruyama[1], Toshiko Ohta[1] and Kunio Takeyasu[2]

[1]Institute of Basic Medical Sciences, Graduate school of comprehensive human sciences, University of Tsukuba, Tennoh-dai, Tsukuba 305-8575, Japan
[2]Laboratory of Plasma Membrane and Nuclear Signaling, Graduate School of Biostudies, Kyoto University, Sakyo-ku, Kyoto 606-8502, Japan

Running title: nucleoid compaction by oxidative stress

*Corresponding author: Kazuya Morikawa, PhD.
Institute of Basic Medical Sciences,
Graduate school of comprehensive human sciences,
University of Tsukuba, Tennoh-dai, Tsukuba 305-8575, Japan
Phone & fax: +81-29-853-3928
e-mail: morikawa@sakura.cc.tsukuba.ac.jp

Key words: AFM, nucleoid, oxidative-stress, *Staphylococcus aureus*, MrgA

Total character: 50573

Abstract

A single-molecule-imaging technique, atomic force microscopy (AFM) was applied to the analyses of the genome architecture of *Staphylococcus aureus*. The staphylococcal cells on a cover glass were subjected to a mild lysis procedure that had maintained the fundamental structural units in *Escherichia coli* (Kim *et al.*, 2004). The nucleoids were found to consist of fibrous structures with diameters of 80 and 40 nm. This feature was shared with the *E. coli* nucleoid. However, whereas the *E. coli* nucleoid dynamically changed its structure to a highly compacted one towards the stationary phase, the *S. aureus* nucleoid never underwent such a tight compaction under a normal growth condition. Bioinformatic analysis suggested that this was attributable to the lack of IHF that regulate the expression of a nucleoid protein, Dps, required for nucleoid compaction in *E. coli*. On the other hand, under oxidative conditions, MrgA (a staphylococcal Dps homologue) was over-expressed and a drastic compaction of the nucleoid was detected. A knock-out mutant of the gene encoding the transcription factor (*perR*) constitutively expressed *mrgA*, and its nucleoid was compacted without the oxidative stresses. The regulatory mechanisms of Dps/MrgA expression and their biological significance were postulated in relation to the nucleoid compaction.

Introduction

In bacteria, the genomic DNA is packed in a cell as a form of "nucleoid" (Azam *et al.*, 2000; Poplawski & Bernander, 1997; Robinow & Kellenberger, 1994), whereas, in eukaryotic cells, the genomic DNA exists in a form of chromatin and is packed in a nucleus (Wolffe, 1995). In either case, to organize the DNA into higher-order structures, a set of distinct structural DNA binding proteins, such as histones in eukaryotic cells, constitutively play major roles by utilizing the physical/chemical properties of DNA-protein interactions. A number of additional proteins also play crucial roles in the maintenance of well organized higher order structures of chromosome (Hayat & Mancarella, 1995; Swedlow & Hirano, 2003). These compacted genomes of prokaryotes and eukaryotes have known to undergo dynamic structural changes depending upon their activities during the cell cycle. Therefore, it is critical to elucidate the transition mechanisms between the distinct hierarchies of the chromosome organization.

Atomic force microscope (AFM) scans a sample surface with a very sharp probe and reveals the topography of the sample surface (Bustamante *et al.*, 1997; Hansma & Hoh, 1994; Hansma *et al.*, 1988). We have developed a series of procedures for the biological application of AFM (Nettikadan *et al.*, 1996; Ohta *et al.*, 1996; Sato *et al.*, 1999; Yoshimura *et al.*, 2000a; Yoshimura *et al.*, 2000b). In our previous study on the *Escherichia coli* nucleoid (Kim *et al.*, 2004), a hierarchy of 40 nm, 80 nm, and thicker fibers was found to be a key feature for the architecture of the genome organization, and that this hierarchy undergoes a series of changes during the growth. On the basis of these results, a structural model has been proposed for the nucleoid organization (Fig. 1), in which the 80 nm fibers play a role as a fundamental structural unit. The 80 nm fiber builds up a 300 nm loop in cells and a coral reef structure is formed during the progression of cell growth phases. In the previously proposed model (Trun & Marko, 1998), a random coil structure of DNA is turned into a loop domain every 50 kbp. This model could explain the structural relationship between the 300 nm loop and the coral reef structure. The coral reef structure might be composed of a number of 300 nm loops, and undergoes further compaction towards the stationary phase. Mutant analyses revealed that a nucleoid protein, Dps, plays a key role for the nucleoid compaction towards the stationary phase (Kim *et al.*, 2004).

The Dps protein, which is encoded by a gene, *dps*, is a member of the Fe-binding protein family that forms multimers in cells (Grant *et al.*, 1998; Ren *et al.*, 2003). The Dps protein and its homologues have DNA binding activity (Chen & Helmann, 1995; Martinez & Kolter, 1997), and *E. coli* Dps is known to be the dominant nucleoid protein in the stationary phase cells (Talukder *et al.*, 1999). The *dps* gene expression in *E. coli* is up-regulated by a transcription factor, IHF, and the σ^s-factor towards stationary phase (Altuvia *et al.*, 1994; Lomovskaya *et al.*, 1994). Bioinformatic analysis has revealed that not all bacterial species possess the *dps* gene and its regulators; e.g., *Clostridium perfringens* lacks them (Takeyasu *et al.*, 2004). Our preliminary analysis has suggested that, although *Staphylococcus aureus* has a *dps* homologue gene, *mrgA*, the regulatory mechanisms of the nucleoid architecture are quite different from those in *E. coli,* because 40 and 80 nm fibers were still observed at the stationary phase in *S. aureus* (Takeyasu *et al.*, 2004).

In this study, the nucleoid architectures of *S. aureus* were investigated in detail by AFM. The results obtained showed that the *S. aureus* nucleoid always exhibited 40 and 80 nm fibers and was never compacted during a normal growth condition. However, it did undergo drastic conformational changes into a compacted clump under an oxidative stress condition. Bioinformatics on the transcriptional regulators for the *dps* gene and its homologues suggested that the oxidative stress, which is directly sensed by evolutionary distinct regulators, is a common induction signal among bacterial phyla, whereas the stationary phase-specific regulation is rather restricted to some species.

Results

Staphylococcal nucleoids do not undergo a stationary-phase compaction.

A clinical isolate designated N315 was selected as a representative of *S. aureus*, because its defined genomic sequences certify the intactness of the important genes focused in this study (Kuroda *et al.*, 2001).

The *S. aureus* N315v cells, control strain cells, were collected at intervals during their growths, lysed as described in Materials and Methods, and subjected to AFM analyses. The nucleoids from the log- and the late log-phase cells were composed of 40 and 80 nm fibers (Fig. 2C-D). The nucleoids from the cells that had been incubated for

2 days still released the 40 and 80 nm fibers upon lyses (Fig. 2E). This finding suggests that the fundamental fiber-units required to build up the higher-order architectures in *S. aureus* are essentially the same as those in *E. coli*. However, the nucleoids of both species evidently behave differently towards the stationary phase; i.e., the *E. coli* nucleoid undergoes a compaction under a normal growth condition (Kim *et al.*, 2004), but the *S. aureus* nucleoid does not.

MrgA is the key factor in the nucleoid compaction.

We previously demonstrated that the key factor for the nucleoid compaction is the Dps protein in *E. coli* (Kim *et al.*, 2004). In *S. aureus* and other Gram-positive bacteria such as *Bacillus subtilis*, the Dps homologue is designated as MrgA (Metallo regulated genes A), which has a 40% amino acid sequence similarity (23.8% identity) to *E. coli* Dps. Northern blot analyses were used to define the timing when the endogeneous *mrgA* gene can be expressed. In the BHI medium, the *mrgA* gene was expressed at a certain level in the log phase, and this level was rather sustained throughout the growth (Fig. 2F), which is quite different from the case of the *E. coli dps* gene whose expression is drastically up-regulated towards the stationary phase (Azam *et al.*, 1999).

To test whether staphylococcal MrgA is functionally equivalent to *E. coli* Dps in the nucleoid compaction, we examined the effect of MrgA over-expression on the nucleoid structure. The MrgA-over-expressing strain, N315M, was grown in the BHI medium and the nucleoids from the log- and stationary-phase cells were subjected to the AFM analyses (Fig. 3). The fibers released from the cells were hardly detectable. Instead, N315M exhibited a highly clumped structure (Fig 3A-B; 96.6% (n = 59) of N315M and 0% (n = ~ 31) of N315v cells exhibited the clumped structure) which contained DNA as proved by DAPI staining (compare Fig. 3C). These results indicate that an over-expression of MrgA promotes the formation of clumped structure, and suggest that MrgA is the functional counterpart of Dps.

Oxidative stress induces the expression of mrgA and nucleoid compaction.

We searched for certain environmental conditions or stresses that could induce the *mrgA* expression. The *S. aureus* cells grown in the BHI medium until mid-log phase were exposed to different growth conditions or stresses and subjected to a Northern-blot analysis (Fig. 4A). A shift to the oxygen-limiting condition, where *S. aureus* could grow

anaerobically, had no positive effect on the *mrgA* expression. Similarly, other stresses such as a hypotonic shock, a heat shock, a β-lactam antibiotic, and a different culture medium (RPMI1640), had no inducible effect on the *mrgA* expression. In contrast, the oxidative stresses by phenanthrenquinone (PQ), menadione (MD), and H_2O_2 drastically induced the *mrgA* gene expression. This indicates that the reactive oxygen species are effective inducers for the *mrgA* expression. This is expected to promote the nucleoid compaction.

To examine the expected conformational dynamics, the nucleoids from the *S. aureus* cells exposed to the oxidative stresses were subjected to the structural analyses under AFM. During the incubation for 30 min in the presence of the redox-cycling reagent, PQ, the nucleoids underwent a drastic structural change into the clumped complex (Fig. 4B; 100% (n = 32) of the cells treated with PQ exhibited the compacted structure), and the 40 and 80 nm fibers were rarely detected. When the cells were cultured for 2 days under the PQ exposure (Fig. 4C), we could never find the 40 and 80 nm fibrous structures released from the cell.

Other oxidative stresses by MD (data not shown) and H_2O_2 (Fig. 4D) also induced the nucleoid compaction (Percentages of the cells exhibiting the compacted structure is 59.2 (n = 152) and 38.8 (n = 49) for the MD and 50 mM H_2O_2 treatments, respectively.) In contrast, it should be noted that, without the oxidative stress, the nucleoids never underwent such structural changes (Fig. 2). These results indicate that the oxidative stress is a key signal that triggers the MrgA-dependent nucleoid compaction.

The *mrgA* mutant was generated as described in Materials and Methods. The growth rate and colony morphology were not affected by the *mrgA* mutation, indicating that *mrgA* is dispensable in the normal growth condition. However, the *mrgA* mutant could not exert the nucleoid compaction response when exposed to the oxidative stress (Fig. 5A-B). This indicates that *mrgA* gene is essential to construct the compacted nucleoid structure under the oxidative stress. We also confirmed that the *mrgA* mutant exhibited increased susceptibility to H_2O_2 (Fig. 5C) as well as to UV irradiation (Fig. 5D) that can cause direct DNA damage and possibly indirect damage via the production of reactive oxygen species (ROS) (Cadet *et al.*, 2005). Theses results are in line with the previous reports in other species (Nair & Finkel, 2004).

OxyR and PerR, regulators of dps/mrgA, spread widely in the bacterial kingdom.

OxyR and PerR are evolutionarily distinct transcription factors that are known to regulate the expression of *dps* (Altuvia *et al.*, 1994) and *mrgA* (Horsburgh *et al.*, 2001a), respectively, in response to oxidative stresses (see Discussion). OxyR acts as an activator and belongs to the large LysR-family of transcriptional regulators (Schellhorn, 1995), and PerR acts as a repressor and is homologous to Fur and Zur that are different from the LysR-family (Horsburgh *et al.*, 2001a). Phylogeneitc analysis of the LysR-family and the Fur homologs revealed that OxyR and PerR form distinct clades in their phylogenetic trees (Fig. 6A, B). *S. aureus* possess SA2330 and SA2123 as the LysR-family proteins, but they were excluded from the OxyR clade, implying that they may not share the functions with OxyR. When the occurrences of Dps/MrgA (Takeyasu *et al.*, 2004) were compared with those of OxyR and PerR, 85.3 % of the 66 strains containing Dps/MrgA possessed at least one of them, and, interestingly, most species in *Bacillales* and *Lactobacillales* carried PerR, but not OxyR (Table 2). Another transcription factor, IHF, which is known to regulate the *E. coli dps* gene towards the stationary phase (Altuvia *et al.*, 1994), was restricted mostly in Proteobacteria. The PerR was expected as the key regulator in the nucleoid compaction in *S, aureus*.

Based on the above considerations, we examined the effect of the *perR* mutation on the nucleoid structure in *S. aureus*. Our *perR* mutant generated from N315 constitutively expressed the *mrgA* gene in the absence of the oxidative stress (Fig. 7A), as expected. This is consistent with the previous study (Horsburgh *et al.*, 2001a; Morrissey *et al.*, 2004). The growth rate was not altered by the *perR* mutation in the employed growth condition. The nucleoid of the *perR* mutant exhibited the compacted structure in the absence of the oxidative stress, and no fibrous structure was detected (Fig. 7B).

Discussion

AFM combined with the “on-substrate lysis” method revealed that the 80 nm and 40 nm fibers dominated when the nucleoid was released from the *S. aureus* cells at any growth phases (Fig. 2). These fibers were stable, never unfolded further in the present experimental condition, and seem to be the common structural units of bacterial nucleoids, since they have been found in the log phase cells of *S. aureus*, *C. perfringens*

and *E. coli* (Takeyasu *et al.*, 2004). These fibers in *S. aureus* underwent a tight compaction under certain conditions as seen in *E. coli* (Fig. 4). Possible genetic switches for the nucleoid compaction can be proposed where the *dps/mrgA* genes and their products (Dps/MrgA) play a key role under different growth phases and oxidative stresses (Fig. 1, Fig. 3). In *S. aureus*, the nucleoid compaction is thought to hardly hinder the cellular processes required for the normal growth in the employed growth condition; N315M and *perR* mutant cells could grow normally. In addition, loss of the *mrgA* gene did not influence the progression into the stationary phase. This is also true in *E. coli*; the *dps* mutant, which is deficient in constructing higher order nucleoid structures, can enter into the stationary phase (Kim *et al.*, 2004; Nair & Finkel, 2004). Thus, the *dps/mrgA* dependent nucleoid compaction seems to be dispensable in the control of the log-phase to stationary-phase transition itself.

Roles of Dps/MrgA in the oxidative stress resistance

ROS are highly reactive molecules, which are generated during the oxidative respiration of bacteria themselves, leading to damages of various macromolecules including the genomic DNA (Nunoshiba *et al.*, 1999). In our defense system, phagocytes such as neutrophils and macrophages produce ROS to kill the infectious bacteria (Clements & Foster, 1999; El-Benna *et al.*, 2005). On the other hand, bacteria are often equipped with several surviving mechanisms against the oxidative stress. For example, bacterial enzymes such as super oxide dismutase and catalase convert the ROS into safe molecules (Clements *et al.*, 1999; Sanz *et al.*, 2000; Valderas & Hart, 2001). The Dps/MrgA family proteins also constitute the oxidative stress-responsive systems (Almiron *et al.*, 1992; Martinez & Kolter, 1997). The Dps protein is a stress-induced protein with a molecular weight of 19 kDa and is known to be a member of the Fe-binding protein family that forms multimers in cells (Grant *et al.*, 1998). A *dps* homologue, *mrgA* in *B. subtilis* was found as the metal ion responsive gene (Chen *et al.*, 1993). Its product, MrgA, can also form a multimer complex *in vitro* and possibly can bind DNA (Chen & Helmann, 1995). The protective mechanism by Dps/MrgA has been attributed to their ability to reduce the intracellular level of iron (Fe^{2+}) that generates the super oxide anion through the Fenton reaction (Zhao *et al.*, 2002). Alternatively, it has been suggested that their DNA binding might protect the genome against the ROS (Wolf *et al.*, 1999). An additional possible resistance mechanism may be that a reduction of

the nucleoid "surface" by Dps/MrgA-dependent compaction (Fig. 3) reduces the challenges of ROS, although we have no direct evidence for the relationship of the nucleoid compaction and the resistance.

Additional factors regulating the nucleoid compaction

It is surprising that an over-expression of MrgA in *S. aureus* could induce a nucleoid compaction in log-phase cells (Fig. 3A), because an over-expression of Dps in *E. coli* cannot induce such a compaction in the log-phase (Kim *et al.*, 2004). It may be that certain factor(s) that cooperatively functions with MrgA is constitutively active in *S. aureus*. Alternatively, certain inhibitory factor(s) that inhibits the nucleoid compaction may exist in the log-phase *E. coli* cells, but not in *S. aureus*. For the latter case, the candidates may include the *E. coli*-specific components of the nucleoid, such as Fis and H-NS. It is interesting to note that the expression level of Fis declines toward the stationary phase (Ball *et al.*, 1992; Talukder *et al.*, 1999).

It can be speculated that the nucleoid compaction requires a modulation of the DNA superhelical density. In fact, the previous biochemical studies have revealed that oxidative stresses affect the DNA topology (Weinstein-Fischer *et al.*, 2000). Two enzymes, topoisomerase and gyrase, can modulate the superhelical density of DNA in response to the oxidative stresses, and the Fis protein reduces the activity of DNA gyrase and counteracts the increase of the overall superhelicity of DNA during early exponential growth phase (Muskhelishvili & Travers, 2003). It is likely that Fis acts as an inhibitory factor in the nucleoid compaction in *E. coli*, and its counterpart is missing in *S. aureus*.

Regulatory mechanism of the dps/mrgA genes

In *E. coli,* IHF together with σ^s-factor up-regulates the *dps* gene expression towards the stationary phase (Fig. 8) (Altuvia *et al.*, 1994), and the amount of its product, Dps, reaches up to 180,000 molecules/cell (~25-fold induction) (Talukder *et al.*, 1999). In contrast, the staphylococcal *mrgA* gene was not induced toward the stationary phase (Fig. 2F); observation attributable to the lack of the IHF/σ^s system (Takeyasu et al., 2004; Fig. 8). The differences of such regulatory modes are well correlated with the nucleoid compaction status in normal growth condition.

A phylogenetic analysis of LysR family defined the OxyR group as a tight clade (Fig.

6A). The two cystein residues that are essential to form a disulfide bridge within the sensor domain in *E. coli* OxyR (Linke & Jakob, 2003) were conserved in the defined OxyR group proteins, but never found in the other LysR-family proteins. Therefore, it is unlikely that SA2330 and SA2123 are functionally equivalent to OxyR. This is consistent with the fact that the *perR* mutation is sufficient to abolish the oxidative stress-response of the *mrgA* gene expression (compare lanes 3 and 4 in Fig. 7A).

Under oxidative stress, PerR derepresses the *mrgA* gene expression in the presence of iron but not manganese (Horsburgh *et al.*, 2001a; Horsburgh *et al.*, 2002; Morrissey *et al.*, 2004). Fur and Zur are the other members of Fur homologues, and dependent on iron and zinc, respectively (Andrews *et al.*, 2003; Gaballa & Helmann, 1998; Horsburgh *et al.*, 2001b; Patzer & Hantke, 1998). The phylogenetic tree of Fur homologues (Fig. 6B) revealed that *E. coli* lacks PerR but possesses Fur (b0683) and Zur (b4046). However, b0683 and b4046 cannot compensate for the OxyR function in the *dps* gene regulation, i.e., *dps* was not induced under oxidative stress in *Δ*oxyR mutant of *E. coli* in which the *b0683* and *b4046* genes were intact (Zheng *et al.*, 2001).

Namely, *S. aureus* and *E. coli* exclusively utilizes PerR and OxyR, respectively, to regulate the *mrgA/dps* expression as an oxidative stress response (Fig. 8). These systems seem to have evolved independently in Proteobacteria and *Firmicutes* (Table 2).

Bacillus subtilis, a close relative of *S. aureus*, also lacks the *ihf* gene but possesses two *mrgA* genes. One is under a control of PerR (Bsat *et al.*, 1998; Chen & Helmann, 1995; Fuangthong & Helmann, 2003), and the other seems to be regulated by SigB in a growth phase-dependent manner (Antelmann *et al.*, 1997). Although SigB is conserved in *Bacillales*, the *mrgA* genes of *S. aureus, Staphylococcus epidermidis, Oceanobacillus iheyensis, Bacillus anthracis, Bacillus thuringiensis, and Bacillus cereus* harbor no potential sequence that could be recognized by SigB. In fact, staphylococcal *mrgA* was not induced toward the stationary phase (Fig. 2F) in spite of the activation of SigB (Bischoff *et al.*, 2001; Giachino *et al.*, 2001).

In summary, although *Firmicutes* and Proteobacteria have different regulatory systems for the *dps/mrgA* gene expression, they seem to respond to the oxidative stress in a similar fashion (i.e., condensing their nucleoids) via the OxyR and PerR systems, respectively. We suspect that bacteria generally respond to the oxidative stress by constructing highly organized nucleoid architectures, and that the certain species have

acquired the ability to respond to the starvation or stationary phase signals. Extra-ordinal regulatory systems of the nucleoid conformation may be found in species such as *Streptococcus pneumoniae* and *Treponema pallidum* (Table 2) carrying the *dps* genes that are not regulated by OxyR and PerR.

Experimental Procedures

Construction of mrgA overexpressing strain

The *mrgA* gene (*SA1941*, *dps* homologue) of *S. aureus* N315 (a clinical isolate in 1982, pre-MRSA (Kuroda *et al.*, 2001; Kuwahara-Arai *et al.*, 1996)) was amplified by PCR with a set of primers, SA1941-f(Eco): 5'-GGAATTCGACAATTTTAAGGAGTGT-3', and SA1941-r(Sal): 5'-CGCGTCGACTGTAGATTAGCTTAAGTAAGA-3'. The SA1941-f(Eco) primer was designed to include the Shine-Dalgarno sequence (double underlined). The amplified 468 bp fragment was digested with *Eco*R I and *Sal* I, and cloned into the *Eco*R I –*Sal* I sites of pRIT5H (Morikawa *et al.*, 2003). The resulting plasmid, pRIT-mrg, can overexpress MrgA under a control of the proteinA promoter. The pRIT-mrg was introduced into the N315 strain to generate a strain, N315M. To generate a control strain, N315v, pRIT5H was introduced into N315. The plasmids were stably maintained in the presence of 12.5 μg/ml chloramphenicol.

Growth condition

Glycerol stocks of *S. aureus* strains (Table 1) were inoculated into Brain-Heart Infusion (BHI) media containing 12.5 μg/ml chloramphenicol and cultured at 37°C with constant shaking (180 rpm) for 24 hr. Three ml of the saturated culture was inoculated into 400 ml of fresh BHI with chloramphenicol and cultured at 37°C with constant shaking to an appropriate cell density. The cell density was determined by measuring the absorbance at 600 nm.

RNA isolation and Northern hybridization analyses

S. aureus strains were grown in drug-free BHI medium until the $O.D._{600}$ reached at 0.5 (log phase), and were exposed to the appropriate stresses for 30 min. Anaerobic condition was made by using AnaeroPack (Mitsubishi Gas Chemical). Oxidative stresses were given by the addition of 20 μM 9,10-phenanthrenquinone (PQ), 80μM

2-methyl-1,4-naphthoquinone (menadione; MD), and 500 μM or 50 mM of H_2O_2. After 30 min incubation, the cells were harvested by a centrifugation at 13,000 x *g* for 30 sec at 4 ˚C, suspended in a lysis buffer containing 10 mM Tris-HCl (pH 8.0), 10 mM EDTA, and 100 μg/ml of lysostaphin, and, then, incubated at 37˚C for 2 min followed by the on-ice incubation for 30 min. The total RNA was extracted from the lysate by the SV total RNA isolation system (Promega). Four μg of the total RNAs was separated on a 1 % agarose-formamide denaturing gel and transferred onto the Hybond N^+ membrane (Amersham Biosciences). The DNA fragments of the *mrgA* gene prepared by PCR from the N315 genomic DNA were labeled by a random priming method using the Ready-to-Go DNA labeling Beads (Amersham Biosciences), and used as the probes. The hybridization was conducted at 60 ˚C in the hybridization solution containing 5 x SSPE, 5 x Denhardt's solution, 0.5 % SDS, and 20 μg/ml of salmon sperm DNA for 16 hr, and the final washing was done at 60 ˚C in 0.1 x SSC and 0.1 % SDS for 30 min.

Bacterial cell lyses procedures

S. aureus cells were harvested from a 500 μl culture by centrifugation (13,000× g, 1min at 4°C) and washed once with 1 ml PBS (pH 7.2). The cells were resuspended in 0.25 ml or 2 ml of PBS and a 5 μl aliquot was placed onto a round-shape cover glass, 18 mm in diameter. The extra liquid was removed by nitrogen gas blow. The sample was immersed in 100 μl of a buffer containing 10 mM Tris-HCl (pH 8.2), and 0.1 M NaCl for 5 min, followed by an sequential addition of 10 μl Lysostaphin (1mg/ml) (Wako, Japan) and 10 μl of 2 mg/ml N-Acetylmuramidase SG (Seikagaku Corporation, Japan). After 2 min incubation at 25°C, Brij 58 (polyoxyethylene hexadecyl ether) and sodium deoxycholate, were added for 10 min to the final concentrations of 0.25 mg /ml and 0.1 mg /ml, respectively. After the specimen was gently washed with distilled water, the excess water on the specimen was removed under nitrogen gas for microscopic analyses.

Microscopy

The atomic force microscope (SPI3800N-SPA400) from Seiko Instrument Inc. was used for the imaging of *S. aureus* nucleoid structures in air at room temperature under a dynamic force mode with a 150 μm scanner. Probes made of a single silicon crystal with the cantilever length of 129 μm and the spring constant of 33–62 N/m

(OMCL-AC160TS-W2, Olympus) were used for imaging. Data was collected in the height mode with a scanning rate of 0.2–0.5 Hz and the driving amplitude of 40–80 mV. The images were captured in a 512 × 512-pixel format and the captured images were flattened and plane-fitted before analysis. The image analyses were performed with the software accompanying with the imaging module (Seiko Instrument Inc., Japan).

All of the AFM images contain "tip effect". The sizes of the objects in the images were estimated at the half maximum height (FWHM; full width at half-maximum) for correction of the tip effect (Schneider *et al.*, 1998). In the present study, we have found that the AFM cantilevers purchased from Olympus had a constant tip angle (~35 degrees) and tip radius (20 nm ± 2 nm) by measuring the apparent width of double stranded DNA in the AFM images.

For the fluorescence microscopy, the sample was incubated in 4',6-diamino-2-phenylindole (DAPI, Sigma) solution (1μg/ml), and observed under a fluorescence microscope (DM RBE, Leica, Germany), and the images were captured by a chilled CCD camera (C5985, Hamamatsu Photonics, Japan).

Construction of mrgA and perR mutants

The *mrgA* targeting vector, pKILts-cat1941, was constructed as follows.

The chloramphenicol acetyl transferase gene (*cat*) including its promoter region was amplified from pRIT5H by PCR with a set of primers CAT(+P)F: 5'-CGAAAATTGGGTACCGTGGGATATTTT-3' and CAT(+T)R: 5'-CAACTAACGGGGCATATGAGTGACATT-3'. The fragment was blunt-ended and cloned into *Sma* I site of pKILts (Morikawa *et al.*, 2001), which has tetracycline resistance marker and the temperature-sensitive replication origin for *S. aureus*. The resulting plasmid was designated pKILts-cat.

The upstream and downstream regions of the *mrgA* gene were amplified by PCR with the primers: UF1941-1: 5'-CCGGATCCTATCGTGAAGGGTTTATTAC-3' and UF1941-2: 5'-GCGGATCCTAATCTAAATGTAAGGTG-3' (for the upstream 1.25 kbp fragment); DF1941-1: 5'-GGCAAGCTTAAGCTAATCTACAGATAAGT-3' and DF1941-2: 5'-GGCAAGCTTTCGCTTCATCGATGATTTG-3' (for the downstream 1.3 kbp fragment). The PCR fragments obtained were sequentially cloned into the *Bam*HI-site and the *Hin*d III-site of pKILts-cat. In the resulting plasmid, pKILts-cat1941, the *cat* gene lies between the two fragments.

The *perR* targeting vector was constructed as follows. The 2.2 kbp region encompassing the *perR* gene was amplified by PCR with a set of primers: UF-perR-1: 5'-GCGGATCCTGAGAGTGACTT-3' and DF-perR-2: 5'-GGCAAGCTTCTCGTCCGTTC-3'. The resultant fragment was blunt-ended and ligated into the *Pvu* II site of pSP72. The *cat* gene was amplified by PCR with the primers, CAT(+P)F and CAT(+T)R (see above), and inserted into the internal *Pvu* II site within the *perR* coding sequence (+136 from the translation initiation site). The fragment encompassing the disrupted *perR* gene was excised from the plasmid by *Bam*H I and *Hin*d III, blunt-ended, and ligated into pKILts to generate the *perR* targeting vector, pKILts-cat-per. This plasmid was passed through a *S. aureus* strain, RN4220, prior to the introduction into N315.

Each of pKILts-cat1941 and pKILts-cat-per was introduced into *S. aureus* N315 by electroporation. The N315 cells carrying the plasmids were grown in BHI containing 10 μg/ml of tetracycline at 30˚C. This growing temperature allows the replication of these plasmids. Then the cells were plated onto a BHI-agar plate containing 12.5 μg/ml of chloramphenicol and incubated at 43˚C in order to select the transformants that had the *cat* gene on its genome. The chloramphenicol resistant colonies were further selected for the absence of the tetracycline resistance by a replica method. These procedures generated the *mrgA* and *perR* mutants, where the original *mrgA* or *perR* gene was replaced with the *cat* gene by a double-cross homologous recombination event. The absence of the *mrgA* or *perR* gene in the mutant was confirmed by PCR.

Oxidative-stress assay

N315 and the *mrgA* mutant cells were washed with PBS. The cells were incubated at 25 ˚C for 3 min in PBS with or without H_2O_2, and then serially diluted with ice-cold saline. The viable cells were counted as colony forming unit (cfu) on BHI agar plates. The assay was independently performed twice, and the representative result was shown in Figure 5C.

UV irradiation

N315 and the *mrgA* mutant cells were serially diluted with ice-cold saline, and plated on BHI agar. The plates were placed under a germicidal lamp (254nm, National GL-15), and exposed for 0 ~ 60 sec. The assay was independently performed twice, and the

representative result was shown in Figure 5D.

Database search

For the 97 bacteria whose genome projects had been completed, the genes encoding OxyR, and PerR were searched within the SSDB (Kanehisa & Goto, 2000). When the genes were not found in certain species, FASTA search of the genes and genomes was conducted on the KEGG database (Kanehisa & Goto, 2000) using the amino acid sequences for OxyR of *E. coli*, and PerR of *S. aureus* and *Synechocystis sp* as queries.

The amino acid sequences of the 879 retrieved proteins homologous to OxyR (e-value is under e-10) and 219 retrieved proteins homologous to PerR (e-value is under 0.0001) were aligned with the ClustalX program (Jeanmougin *et al.*, 1998). The alignment was used for the phylogenetic analysis with the PROTDIST and NEIGHBOUR programs of the PHYLIP 3.6 package (Felsenstein, 1989). The phylogenetic tree was inferred by the neighbour-joining method (Saitou & Nei, 1987) and tested by 1000 replications of the bootstrap analysis which was carried out with the SEQBOOT and CONSENSE programs in the same package, and, then, visualized using the TREEVIEW program (Page, 1996).

Acknowledgements: This study was supported by the Special Co-ordination Funds, the COE Research Grant and the Basic Research Grant (B) from the Ministry of Education, Culture, Sports, Science and Technology of Japan. We thank the Japan Science Society (the Sasakawa Scientific Research Grant) and the Sumitomo Foundation for their strong support for this work.

References

Almiron, M., Link, A. J., Furlong, D., & Kolter, R. (1992). A novel DNA-binding protein with regulatory and protective roles in starved *Escherichia coli*. *Genes Dev* **6**, 2646-2654.

Altuvia, S., Almiron, M., Huisman, G., Kolter, R., & Storz, G. (1994). The *dps* promoter is activated by OxyR during growth and by IHF and sigma S in stationary phase. *Mol Microbiol* **13**, 265-272.

Andrews, S. C., Robinson, A. K., & Rodriguez-Quinones, F. (2003). Bacterial iron homeostasis. *FEMS Microbiol Rev* **27**, 215-237.

Antelmann, H., Engelmann, S., Schmid, R., Sorokin, A., Lapidus, A., & Hecker, M. (1997). Expression of a stress- and starvation-induced *dps/pexB*-homologous gene is controlled by the alternative sigma factor σ^B in *Bacillus subtilis*. *J Bacteriol* **179**, 7251-7256.

Azam, T. A., Hiraga, S., & Ishihama, A. (2000). Two types of localization of the DNA-binding proteins within the *Escherichia coli* nucleoid. *Genes Cells* **5**, 613-626.

Azam, T. A., Iwata, A., Nishimura, A., Ueda, S., & Ishihama, A. (1999). Growth phase-dependent variation in protein composition of the *Escherichia coli* nucleoid. *J Bacteriol* **181**, 6361-6370.

Ball, C. A., Osuna, R., Ferguson, K. C., & Johnson, R. C. (1992). Dramatic changes in Fis levels upon nutrient upshift in *Escherichia coli*. *J Bacteriol* **174**, 8043-8056.

Bischoff, M., Entenza, J. M., & Giachino, P. (2001). Influence of a functional *sigB* operon on the global regulators *sar* and *agr* in *Staphylococcus aureus*. *J Bacteriol* **183**, 5171-5179.

Bsat, N., Herbig, A., Casillas-Martinez, L., Setlow, P., & Helmann, J. D. (1998). *Bacillus subtilis* contains multiple Fur homologues: identification of the iron uptake (Fur) and peroxide regulon (PerR) repressors. *Mol Microbiol* **29**, 189-198.

Bustamante, C., Zuccheri, G., Leuba, S. H., Yang, G., & Samori, B. (1997). Visualization and analysis of chromatin by scanning force microscopy. *Methods* **12**, 73-83.

Cadet, J., Sage, E., & Douki, T. (2005). Ultraviolet radiation-mediated damage to cellular DNA. *Mutat Res* **571**, 3-17.

Chen, L., & Helmann, J. D. (1995). *Bacillus subtilis* MrgA is a Dps(PexB) homologue: evidence for metalloregulation of an oxidative-stress gene. *Mol Microbiol* **18**,

295-300.

Chen, L., James, L. P., & Helmann, J. D. (1993). Metalloregulation in *Bacillus subtilis*: isolation and characterization of two genes differentially repressed by metal ions. *J Bacteriol* **175**, 5428-5437.

Choi, H., Kim, S., Mukhopadhyay, P.*, et al*. (2001). Structural basis of the redox switch in the OxyR transcription factor. *Cell* **105**, 103-113.

Clements, M. O., & Foster, S. J. (1999). Stress resistance in *Staphylococcus aureus*. *Trends Microbiol* **7**, 458-462.

Clements, M. O., Watson, S. P., & Foster, S. J. (1999). Characterization of the major superoxide dismutase of *Staphylococcus aureus* and its role in starvation survival, stress resistance, and pathogenicity. *J Bacteriol* **181**, 3898-3903.

El-Benna, J., Dang, P. M., Gougerot-Pocidalo, M. A., & Elbim, C. (2005). Phagocyte NADPH oxidase: a multicomponent enzyme essential for host defenses. *Arch Immunol Ther Exp (Warsz)* **53**, 199-206.

Felsenstein, J. (1989). PHYLIP-Phylogeny inference package version 3.2. *Cladistics* **5**, 164-166.

Fuangthong, M., & Helmann, J. D. (2003). Recognition of DNA by three ferric uptake regulator (Fur) homologs in *Bacillus subtilis*. *J Bacteriol* **185**, 6348-6357.

Gaballa, A., & Helmann, J. D. (1998). Identification of a zinc-specific metalloregulatory protein, Zur, controlling zinc transport operons in *Bacillus subtilis*. *J Bacteriol* **180**, 5815-5821.

Giachino, P., Engelmann, S., & Bischoff, M. (2001). σ^B activity depends on RsbU in *Staphylococcus aureus*. *J Bacteriol* **183**, 1843-1852.

Grant, R. A., Filman, D. J., Finkel, S. E., Kolter, R., & Hogle, J. M. (1998). The crystal structure of Dps, a ferritin homolog that binds and protects DNA. *Nat Struct Biol* **5**, 294-303.

Hansma, H. G., & Hoh, J. H. (1994). Biomolecular imaging with the atomic force microscope. *Annu Rev Biophys Biomol Struct* **23**, 115-139.

Hansma, P. K., Elings, V. B., Marti, O., & Bracker, C. E. (1988). Scanning tunneling microscopy and atomic force microscopy: application to biology and technology. *Science* **242**, 209-216.

Hayat, M. A., & Mancarella, D. A. (1995). Nucleoid proteins. *Micron* **26**, 461-480.

Horsburgh, M. J., Clements, M. O., Crossley, H., Ingham, E., & Foster, S. J. (2001a).

PerR controls oxidative stress resistance and iron storage proteins and is required for virulence in *Staphylococcus aureus*. *Infect Immun* **69**, 3744-3754.

Horsburgh, M. J., Ingham, E., & Foster, S. J. (2001b). In *Staphylococcus aureus*, *fur* is an interactive regulator with PerR, contributes to virulence, and Is necessary for oxidative stress resistance through positive regulation of catalase and iron homeostasis. *J Bacteriol* **183**, 468-475.

Horsburgh, M. J., Wharton, S. J., Karavolos, M., & Foster, S. J. (2002). Manganese: elemental defence for a life with oxygen. *Trends Microbiol* **10**, 496-501.

Jeanmougin, F., Thompson, J. D., Gouy, M., Higgins, D. G., & Gibson, T. J. (1998). Multiple sequence alignment with Clustal X. *Trends Biochem Sci* **23**, 403-405.

Kanehisa, M., & Goto, S. (2000). KEGG: kyoto encyclopedia of genes and genomes. *Nucleic Acids Res* **28**, 27-30.

Kim, J., Yoshimura, S. H., Hizume, K., Ohniwa, R. L., Ishihama, A., & Takeyasu, K. (2004). Fundamental structural units of the *Escherichia coli* nucleoid revealed by atomic force microscopy. *Nucleic Acids Res* **32**, 1982-1992.

Kreiswirth, B. N., Lofdahl, S., Betley, M. J., *et al*. (1983). The toxic shock syndrome exotoxin structural gene is not detectably transmitted by a prophage. *Nature* **305**, 709-712.

Kuroda, M., Ohta, T., Uchiyama, I., *et al*. (2001). Whole genome sequencing of meticillin-resistant *Staphylococcus aureus*. *Lancet* **357**, 1225-1240.

Kuwahara-Arai, K., Kondo, N., Hori, S., Tateda-Suzuki, E., & Hiramatsu, K. (1996). Suppression of methicillin resistance in a *mecA*-containing pre-methicillin-resistant *Staphylococcus aureus* strain is caused by the *mecI*-mediated repression of PBP 2' production. *Antimicrob Agents Chemother* **40**, 2680-2685.

Linke, K., & Jakob, U. (2003). Not every disulfide lasts forever: disulfide bond formation as a redox switch. *Antioxid Redox Signal* **5**, 425-434.

Lomovskaya, O. L., Kidwell, J. P., & Matin, A. (1994). Characterization of the sigma 38-dependent expression of a core *Escherichia coli* starvation gene, *pexB*. *J Bacteriol* **176**, 3928-3935.

Martinez, A., & Kolter, R. (1997). Protection of DNA during oxidative stress by the nonspecific DNA-binding protein Dps. *J Bacteriol* **179**, 5188-5194.

Morikawa, K., Inose, Y., Okamura, H., *et al*. (2003). A new staphylococcal sigma factor in the conserved gene cassette: functional significance and implication for the

evolutionary processes. *Genes Cells* **8**, 699-712.

Morikawa, K., Maruyama, A., Inose, Y., Higashide, M., Hayashi, H., & Ohta, T. (2001). Overexpression of sigma factor, σ^B, urges *Staphylococcus aureus* to thicken the cell wall and to resist β-lactams. *Biochem Biophys Res Commun* **288**, 385-389.

Morrissey, J. A., Cockayne, A., Brummell, K., & Williams, P. (2004). The staphylococcal ferritins are differentially regulated in response to iron and manganese and via PerR and Fur. *Infect Immun* **72**, 972-979.

Muskhelishvili, G., & Travers, A. (2003). Transcription factor as a topological homeostat. *Front Biosci* **8**, d279-285.

Nair, S., & Finkel, S. E. (2004). Dps protects cells against multiple stresses during stationary phase. *J Bacteriol* **186**, 4192-4198.

Nettikadan, S., Tokumasu, F., & Takeyasu, K. (1996). Quantitative analysis of the transcription factor AP2 binding to DNA by atomic force microscopy. *Biochem Biophys Res Commun* **226**, 645-649.

Nunoshiba, T., Obata, F., Boss, A. C., *et al*. (1999). Role of iron and superoxide for generation of hydroxyl radical, oxidative DNA lesions, and mutagenesis in *Escherichia coli*. *J Biol Chem* **274**, 34832-34837.

Ohta, T., Nettikadan, S., Tokumasu, F., *et al*. (1996). Atomic force microscopy proposes a novel model for stem-loop structure that binds a heat shock protein in the *Staphylococcus aureus* HSP70 operon. *Biochem Biophys Res Commun* **226**, 730-734.

Page, R. D. (1996). TreeView: an application to display phylogenetic trees on personal computers. *Comput Appl Biosci* **12**, 357-358.

Patzer, S. I., & Hantke, K. (1998). The ZnuABC high-affinity zinc uptake system and its regulator Zur in *Escherichia coli*. *Mol Microbiol* **28**, 1199-1210.

Poplawski, A., & Bernander, R. (1997). Nucleoid structure and distribution in thermophilic Archaea. *J Bacteriol* **179**, 7625-7630.

Ren, B., Tibbelin, G., Kajino, T., Asami, O., & Ladenstein, R. (2003). The multi-layered structure of Dps with a novel di-nuclear ferroxidase center. *J Mol Biol* **329**, 467-477.

Robinow, C., & Kellenberger, E. (1994). The bacterial nucleoid revisited. *Microbiol Rev* **58**, 211-232.

Saitou, N., & Nei, M. (1987). The neighbor-joining method: a new method for reconstructing phylogenetic trees. *Mol Biol Evol* **4**, 406-425.

Sanz, R., Marin, I., Ruiz-Santa-Quiteria, J. A., *et al*. (2000). Catalase deficiency in

Staphylococcus aureus subsp. *anaerobius* is associated with natural loss-of-function mutations within the structural gene. *Microbiology* **146 (Pt 2)**, 465-475.

Sato, M. H., Ura, K., Hohmura, K. I., *et al*. (1999). Atomic force microscopy sees nucleosome positioning and histone H1-induced compaction in reconstituted chromatin. *FEBS Lett* **452**, 267-271.

Schellhorn, H. E. (1995). Regulation of hydroperoxidase (catalase) expression in *Escherichia coli*. *FEMS Microbiol Lett* **131**, 113-119.

Schneider, S. W., Larmer, J., Henderson, R. M., & Oberleithner, H. (1998). Molecular weights of individual proteins correlate with molecular volumes measured by atomic force microscopy. *Pflugers Arch* **435**, 362-367.

Swedlow, J. R., & Hirano, T. (2003). The making of the mitotic chromosome: modern insights into classical questions. *Mol Cell* **11**, 557-569.

Takeyasu, K., Kim, J., Ohniwa, R. L., *et al*. (2004). Genome architecture studied by nanoscale imaging: analyses among bacterial phyla and their implication to eukaryotic genome folding. *Cytogenet Genome Res* **107**, 38-48.

Talukder, A. A., Iwata, A., Nishimura, A., Ueda, S., & Ishihama, A. (1999). Growth phase-dependent variation in protein composition of the *Escherichia coli* nucleoid. *J Bacteriol* **181**, 6361-6370.

Trun, N. Y., & Marko, J. F. (1998). Architecture of a bacterial chromosome. *Asm News* **64**, 276-283.

Valderas, M. W., & Hart, M. E. (2001). Identification and characterization of a second superoxide dismutase gene (*sodM*) from *Staphylococcus aureus*. *J Bacteriol* **183**, 3399-3407.

Weinstein-Fischer, D., Elgrably-Weiss, M., & Altuvia, S. (2000). *Escherichia coli* response to hydrogen peroxide: a role for DNA supercoiling, topoisomerase I and Fis. *Mol Microbiol* **35**, 1413-1420.

Wolf, S. G., Frenkiel, D., Arad, T., Finkel, S. E., Kolter, R., & Minsky, A. (1999). DNA protection by stress-induced biocrystallization. *Nature* **400**, 83-85.

Wolffe, A. P. (1995). Centromeric chromatin. Histone deviants. *Curr Biol* **5**, 452-454.

Yoshimura, S. H., Ohniwa, R. L., Sato, M. H., *et al*. (2000a). DNA phase transition promoted by replication initiator. *Biochemistry* **39**, 9139-9145.

Yoshimura, S. H., Yoshida, C., Igarashi, K., & Takeyasu, K. (2000b). Atomic force microscopy proposes a 'kiss and pull' mechanism for enhancer function. off. *J*

Electron Microsc (Tokyo) **49**, 407-413.

Zhao, G., Ceci, P., Ilari, A.*, et al*. (2002). Iron and hydrogen peroxide detoxification properties of DNA-binding protein from starved cells. A ferritin-like DNA-binding protein of *Escherichia coli*. *J Biol Chem* **277**, 27689-27696.

Zheng, M., Wang, X., Templeton, L. J., Smulski, D. R., LaRossa, R. A., & Storz, G. (2001). DNA microarray-mediated transcriptional profiling of the *Escherichia coli* response to hydrogen peroxide. *J Bacteriol* **183**, 4562-4570.

Table 1. *S. aureus* strains used in this study.

Table 2. Prevalence of OxyR and PerR homologues. The OxyR and PerR homologues were defined as the members in the OxyR clade in Figure 6A, and the PerR clade in Figure 6B, respectively. The Dps distribution was derived from our previous analyses (Kim *et al*., 2004; Takeyasu *et al*., 2004).

Figure legends

Figure 1. A model of the architectural hierarchy in *E. coli* nucleoid (Kim *et al.*, 2004). The DNA and nucleoid proteins form a 40 nm fiber structure. The 40 nm fiber is super-solenoided into an 80 nm fiber (their AFM image is shown in left panel). These fiber structures are commonly found in the bacterial nucleoid. The 80 nm fiber, then, forms a loop structure (middle panel, arrows). The nucleoid undergoes a series of drastic structural changes into a tightly compacted state (right panel). The nucleoid compaction is mainly mediated via a nucleoid protein, Dps. In the present study, the loop and coral reef structures were not detected in *S. aureus*. Scale bars, 500 nm.

Figure 2. A-E: Nucleoid structures of *S. aureus* in a normal growth condition. Cells were collected in the mid-log phase (C), late-log phase (D), and stationary phase (E), lysed as described in Materials and Methods and subjected to AFM analyses. The sampling points were marked by arrow heads on the growth curve (A). Close observations of the stationary phase nucleoid showed two different fiber structures (40 and 80 nm). The dotted square areas (C-E) were directly rescanned at higher resolutions and shown as inlets. A curve obtained by a Gaussian fitting was overlaid in the distribution histogram of the fiber widths (bin size, 10 nm) (B). Scale bars, 500 nm. **F**: Northern-blot analysis of the *mrgA* transcripts. N315 cells were harvested at various growth phases. Lanes 1 through 3: O.D.600 = 0.5, 1.0, 1.5, respectively. Lanes 4 through 10: 6, 7.5, 9, 10.5, 12, 26, and 48 hr after inoculation, respectively. The expression of *mrgA* was constitutive throughout the growth. Note that the lane 1 is identical to the lane 1 in Figure 4A. The bottom panel: Ethidium bromide staining of rRNAs.

Figure 3. Nucleoid compaction induced by MrgA overexpression. N315M cells harboring the *mrgA*-expression plasmids were collected in the mid-log phase (A), and

the stationary phase (B), lysed as described in Materials and Methods and subjected to AFM analyses. The dotted square areas were directly rescanned at higher resolutions and shown as inlets. Scale bars, 500 nm. Panels in C are the DAPI-stained images of the lysed cells of N315M and N315v. Scale bars, 20μm.

Figure 4. A: Drastic induction of the *mrgA* expression by oxidative stresses. N315 cells were grown in BHI media until the mid-log phase (lane 1) and exposed to stresses: anaerobic condition (lane 2), heat shock (46 ˚C, lane 3), osmotic stress by 1.5M NaCl (lane 4), oxidative stresses by 80 μM of MD (lane 5), by 20 μM PQ (lane 6), by 500 μM H_2O_2 (lane 7), by 50 mM H_2O_2(lane 10), 16 μg/ml (sub-MIC) of oxacillin (β-lactam antibiotics, lane 8), different medium (RPMI 1640, lane 9) for 30 min. Four μg of the total RNAs were subjected to the Northern-blot analysis with a *mrgA* specific probe (see Materials and Methods). Ethidium bromide staining of rRNAs shows equal loading of RNA. **B-D:** Oxidative stress-induced nucleoid compaction. Cells were grown in BHI media as in Figure 2, but exposed to the oxidative stress by adding 20 μM of PQ (B-C), or 50mM H_2O_2 (D) when $O.D._{600}$ reached 0.5. The cells were harvested after 30 min (B, D) or 2 days (C), and, then, their nucleoids were subjected to the AFM analysis.

Figure 5. A-B: Nucleoid images of the *mrgA* mutant under oxidative stress. The *mrgA* null mutant was exposed to the oxidative stress by adding 20 μM of PQ when $O.D._{600}$ reached 0.5. The cells were harvested after 30 min, and their nucleoids were subjected to the AFM analysis (**A**) or the fluorescent microscopy by DAPI-staining (**B**). Scale bars, 500 nm in A, and 20 μm in B. **C-D**: Increased susceptibilities to oxidative stress and UV irradiation in *mrgA* mutant. **C**: Viabilities of cells after the 200 mM or 400 mM H_2O_2 treatment. N315: open column, *mrgA* mutant: filled column. **D**: UV tolerance. Cells were evenly spread on the BHI-agar plate, and UV was irradiated for the indicated periods. The plate was incubated at 37˚C for overnight to detect colonies from survived cells. The *mrgA* mutant (right) was more susceptible to UV than N315 (left).

Figure 6. Phylogenetic analyses of the LysR family and the Fur homologues. **A**: 879 OxyR homologues. The OxyR clade (red) was clearly separated from other LysR family proteins. The essential cystein residues (199^{th} and 208^{th} from N-terminal) required to form the sensor disulfide bridge (Choi *et al.*, 2001) were conserved in the defined OxyR

clade (BRA0709 in *Brucella meltensis* and BMEII0576 in *Brucella suis* lack 208th Cys), and never found in other LysR family proteins including SA2330 and SA2123. **B:** 219 Fur homologues. The genes identified are colored red in *E. coli*, blue in *B. subtilis* and green in *S. aureus*.

Figure 7. Effect of *perR* mutation on *mrgA* expression and nucleoid structure. **A**: The *perR* mutant expresses *mrgA* without the oxidative stress. N315 (lanes 1 and 2) and the *perR* mutant cells (lanes 3 and 4) were grown in BHI until mid-log phase (lanes 1 and 3), and exposed to 20 μM PQ for 30 min (lanes 2 and 4). Four μg of the total RNAs were subjected to the Northern-blot analysis with the *mrgA* specific probe. Lower panel: Ethidium bromide staining of rRNAs. **B**: Nucleoid image of the *perR* mutant under normal growth condition. Dotted square area was directly rescanned at the higher resolution, and shown as inlet. Scale bars, 500 nm.

Figure 8. Schematic representation of the regulatory mechanisms of the *dps/mrgA* genes in *E. coli* and *S. aureus*. In *E. coli*, IHF and σ^s-factor regulate the *dps* gene expression towards the stationary phase, and OxyR and σ^{70} stimulate the *dps* gene expression under the H_2O_2 stress. In *S. aureus*, only the PerR/(σ^A) pathway exists due to the lack of the genes for IHF/σ^s in the genome. Therefore, the staphylococcal *mrgA* gene cannot be induced toward the stationary phase, although it is expressed under oxidative stresses.

Table 1

Strain	Description	Reference
N315	wild-type strain	Kuwahara-Arai et al., 1996
N315v	vector control, N315 (pRIT5H)	Morikawa et al., 2003
N315M	*mrgA* overexpression, N315 (pRIT-mrg)	This study
N315-ΔmrgA	*mrgA* knockout from N315	This study
N315-ΔperR	*perR* knockout from N315	This study
RN4220	Restriction deficient transformation recipient	Kreiswirth et al., 1983

Table 2

			DPS	OxyR clade	PerR clade
Proteobacteria	gamma	*Escherichia coli K-12 MG1655*	+	+	-
		Escherichia coli K-12 W3110	+	+	-
		Escherichia coli O157 EDL933	+	+	-
		Escherichia coli O157 Sakai	+	+	-
		Escherichia coli CFT073	+	+	-
		Salmonella typhi CT18	+	+	-
		Salmonella typhimurium	+	+	-
		Yersinia pestis CO92	+	+	-
		Yersinia pestis KIM	+	+	-
		Shigella flexneri 301 (serotype 2a)	+	+	-
		Buchnera sp. APS (Acyrthosiphon pisum)	-	-	-
		Buchnera aphidicola (Schizaphis graminu	-	-	-
		Buchnera aphidicola (Baizongia pistaciae,	-	-	-
		Wigglesworthia brevipalpis	-	-	-
		Haemophilus influenzae	+	+	-
		Pasteurella multocida	+	+	-
		Xylella fastidiosa 9a5c	+	+	-
		Xylella fastidiosa Temecula1	+	+	-
		Xanthomonas campestris	+	+	-
		Xanthomonas axonopodis	+	+	-
		Vibrio cholerae	+	+	-
		Vibrio vulnificus	+	+	-
		Vibrio parahaemolyticus	+	+	-
		Pseudomonas aeruginosa	+	+	-
		Shewanella oneidensis	+	+	-
		Coxiella burnetii	-	+	-
	beta	*Neisseria meningitidis MC58 (serogroup B*	-	+	-
		Neisseria meningitidis Z2491 (serogroup A	-	+	-
		Ralstonia solanacearum	+	+	-
	delta/epsil	*Helicobacter pylori 26695*	+	-	-
		Helicobacter pylori J99	+	-	-
		Campylobacter jejuni	+	-	-
	alpha	*Rickettsia prowazekii*	+	-	-
		Rickettsia conorii	-	-	-
		Mesorhizobium loti	-	+	+
		Sinorhizobium meliloti	-	+	+
		Agrobacterium tumefaciens C58 (UWash/I	+	+	+
		Agrobacterium tumefaciens C58 (Cereon)	+	+	+
		Brucella melitensis	+	++	++
		Brucella suis	+	+	++
		Bradyrhizobium japonicum	+	+	++
		Caulobacter crescentus	+	+	-
Firmicutes	Bacillales	*Bacillus subtilis*	+	-	+
		Bacillus halodurans	+	-	+
		Bacillus anthracis	+	-	+
		Bacillus cereus	+	-	+
		Oceanobacillus iheyensis	+	-	+
		Staphylococcus aureus N315 (MRSA)	+	-	+

		Staphylococcus aureus Mu50 (VRSA)	+	-	+
		Staphylococcus aureus MW2	+	-	+
		Staphylococcus epidermidis	+	-	+
		Listeria monocytogenes	+	-	+
		Listeria innocua	+	-	+
	Lactobacil	*Lactococcus lactis*	+	-	+
		Streptococcus pyogenes SF370 (serotype M	+	-	+
		Streptococcus pyogenes MGAS8232 (serot	+	-	+
		Streptococcus pyogenes MGAS315 (seroty	+	-	+
		Streptococcus pneumoniae TIGR4	+	-	-
		Streptococcus pneumoniae R6	+	-	-
		Streptococcus mutans	+	-	+
		Lactobacillus plantarum	+	-	+
		Enterococcus faecalis	+	-	+
	Clostridia	*Clostridium acetobutylicum*	-	-	+
		Clostridium perfringens	-	-	+
		Clostridium tetani	+	-	+
		Thermoanaerobacter tengcongensis	-	-	+
	Mollicutes	*Mycoplasma genitalium*	-	-	-
		Mycoplasma pneumoniae	-	-	-
		Mycoplasma pulmonis	+	-	-
		Mycoplasma penetrans	-	-	-
		Ureaplasma urealyticum	-	-	-
Actinobacteria		*Mycobacterium tuberculosis H37Rv (lab s*	-	-	+
		Mycobacterium tuberculosis CDC1551	-	-	+
		Mycobacterium leprae	-	+	-
		Corynebacterium glutamicum	+	+	-
		Corynebacterium efficiens	+	+	-
		Streptomyces coelicolor	+	+	-
		Bifidobacterium longum	+	-	-
		Tropheryma whipplei Twist	+	-	-
		Tropheryma whipplei TW08/27	+	-	-
Fusobacteria		*Fusobacterium nucleatum*	+	-	-
Chlamydia		*Chlamydia trachomatis*	-	-	-
		Chlamydia muridarum	-	-	+
		Chlamydophila pneumoniae CWL029	-	-	-
		Chlamydophila pneumoniae AR39	-	-	-
		Chlamydophila pneumoniae J138	-	-	-
		Chlamydophila caviae	-	-	-
Spirochete		*Borrelia burgdorferi*	+	-	+
		Treponema pallidum	+	-	-
		Leptospira interrogans	+	-	++
Cyanobacteria		*Synechocystis sp. PCC6803*	+	-	++
		Thermosynechococcus elongatus	+	-	+
		Anabaena sp. PCC7120 (Nostoc sp. PCC7	+	-	+
Green sulfur bacteria		*Chlorobium tepidum*	-	-	-
Radioresistant bacteria		*Deinococcus radiodurans*	+	-	-
Hyperthermophilic bacteria		*Aquifex aeolicus*	-	-	+
		Thermotoga maritima	-	-	+

Figure 1

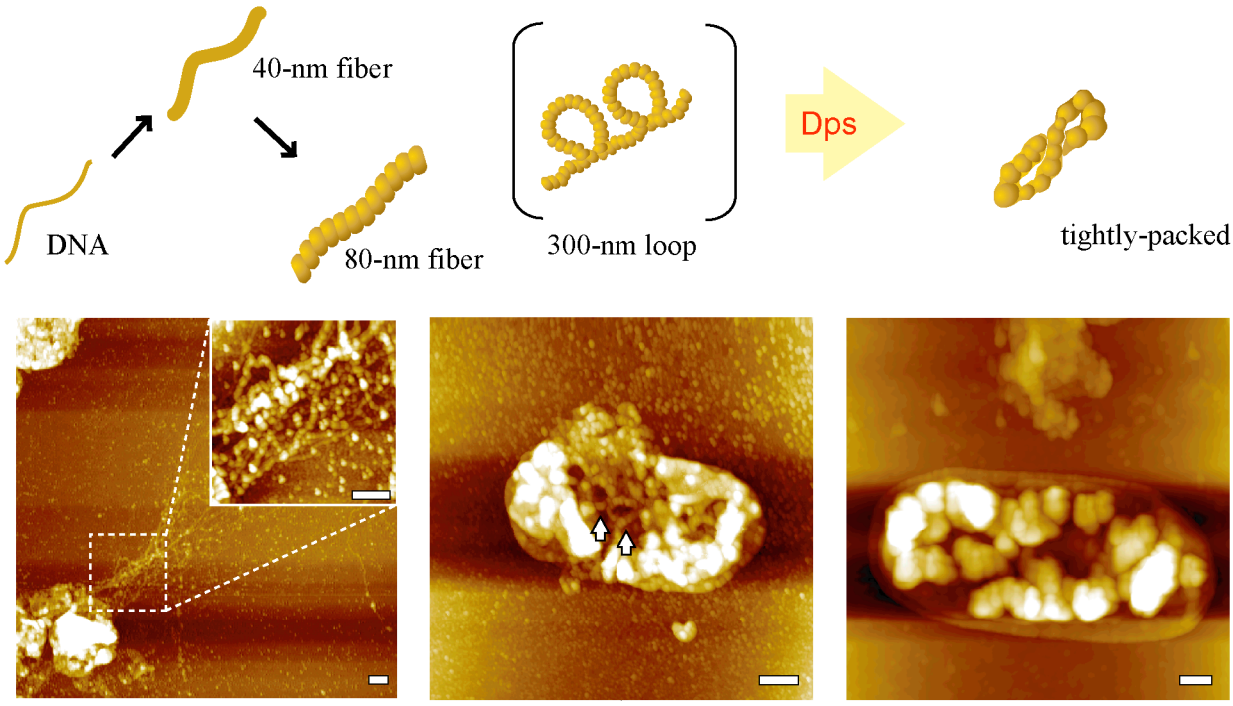

Figure 2

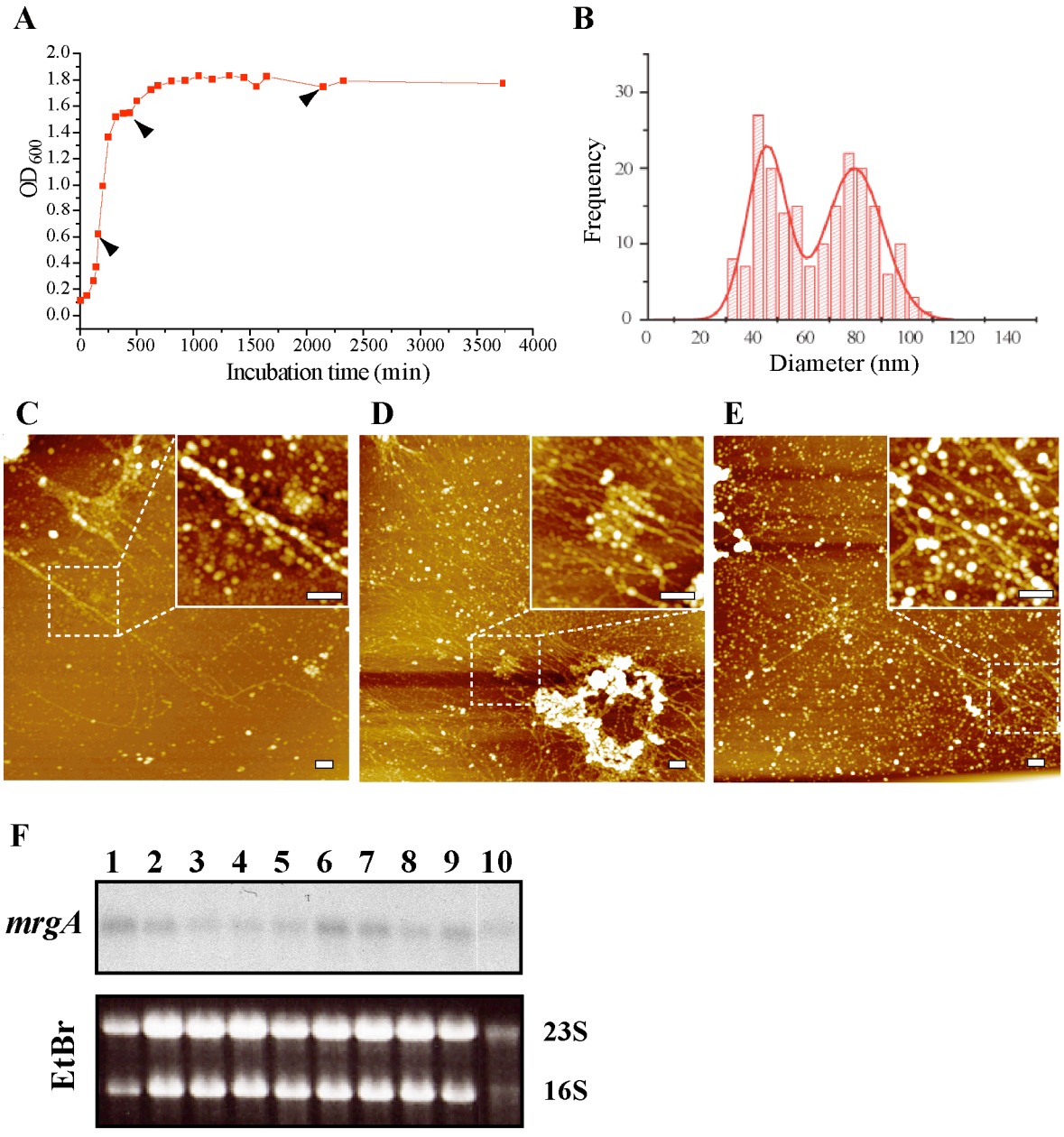
A
B
C
D
E
F
OD600
Incubation time (min)
Frequency
Diameter (nm)
1 2 3 4 5 6 7 8 9 10
mrgA
EtBr
23S
16S

Figure 3

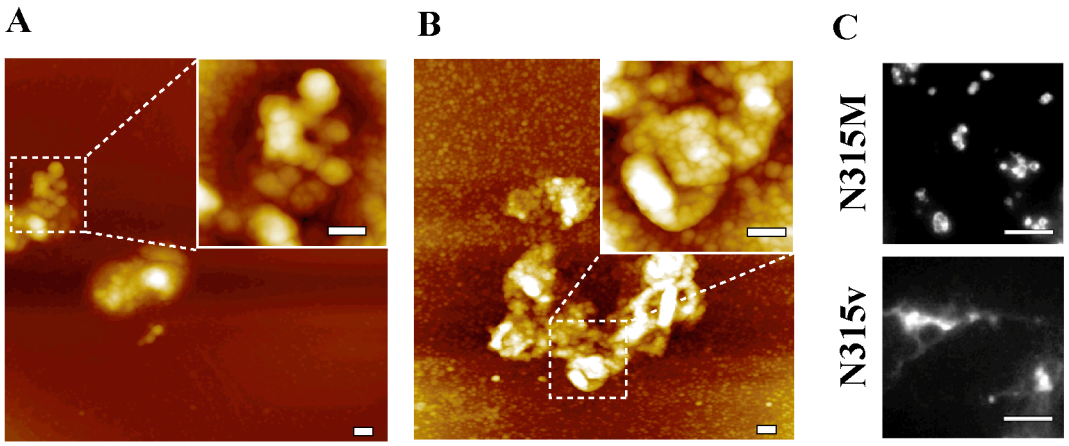

Figure 4

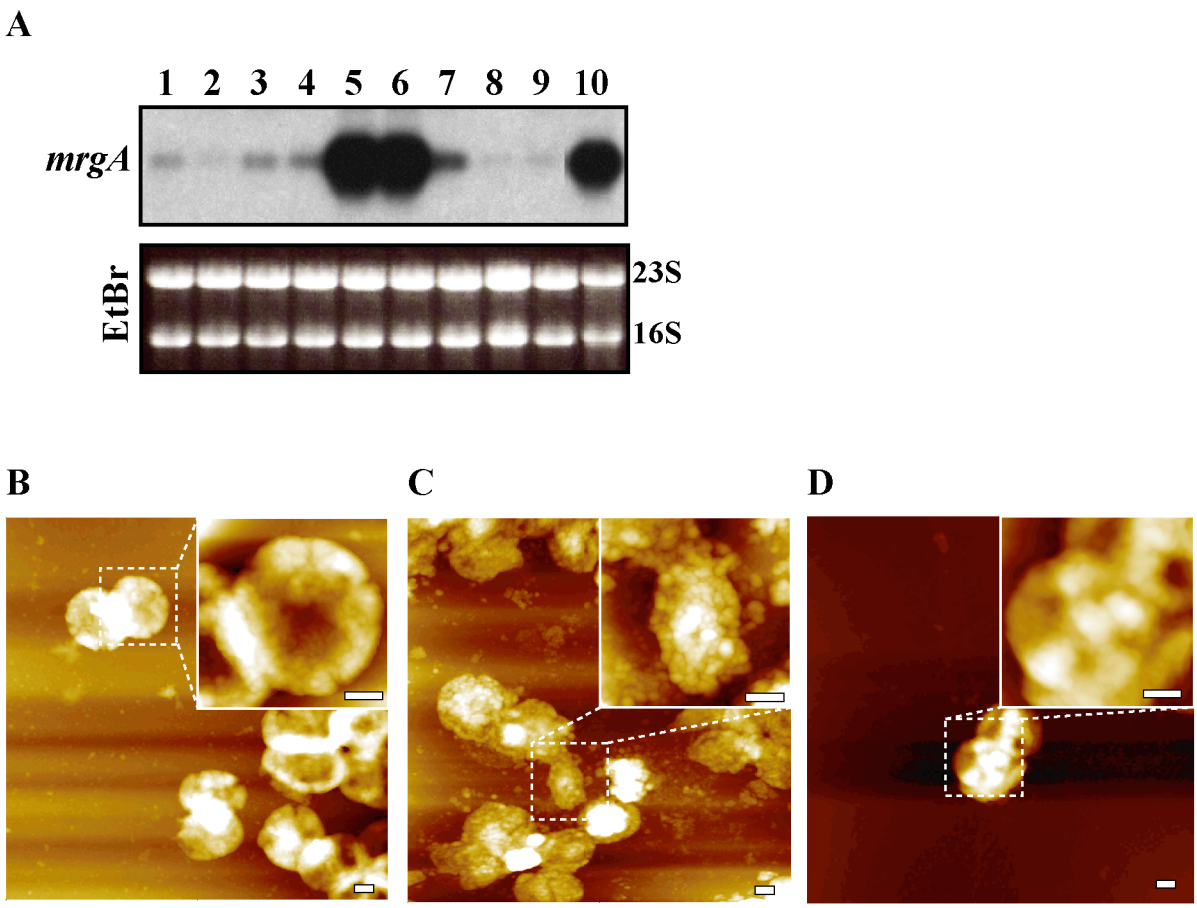

Figure 5

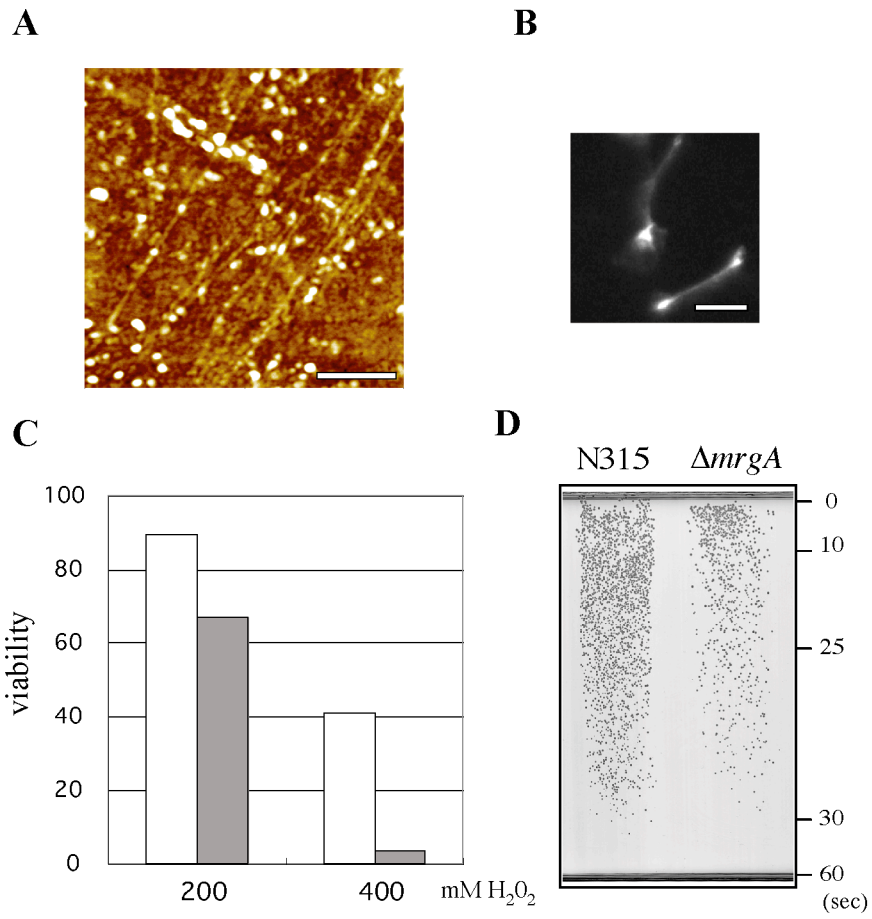
A
B
C
D
100
80
60
40
20
0
viability
200
400
mM H_2O_2
N315
Δ*mrgA*
0
10
25
30
60
(sec)

Figure 6

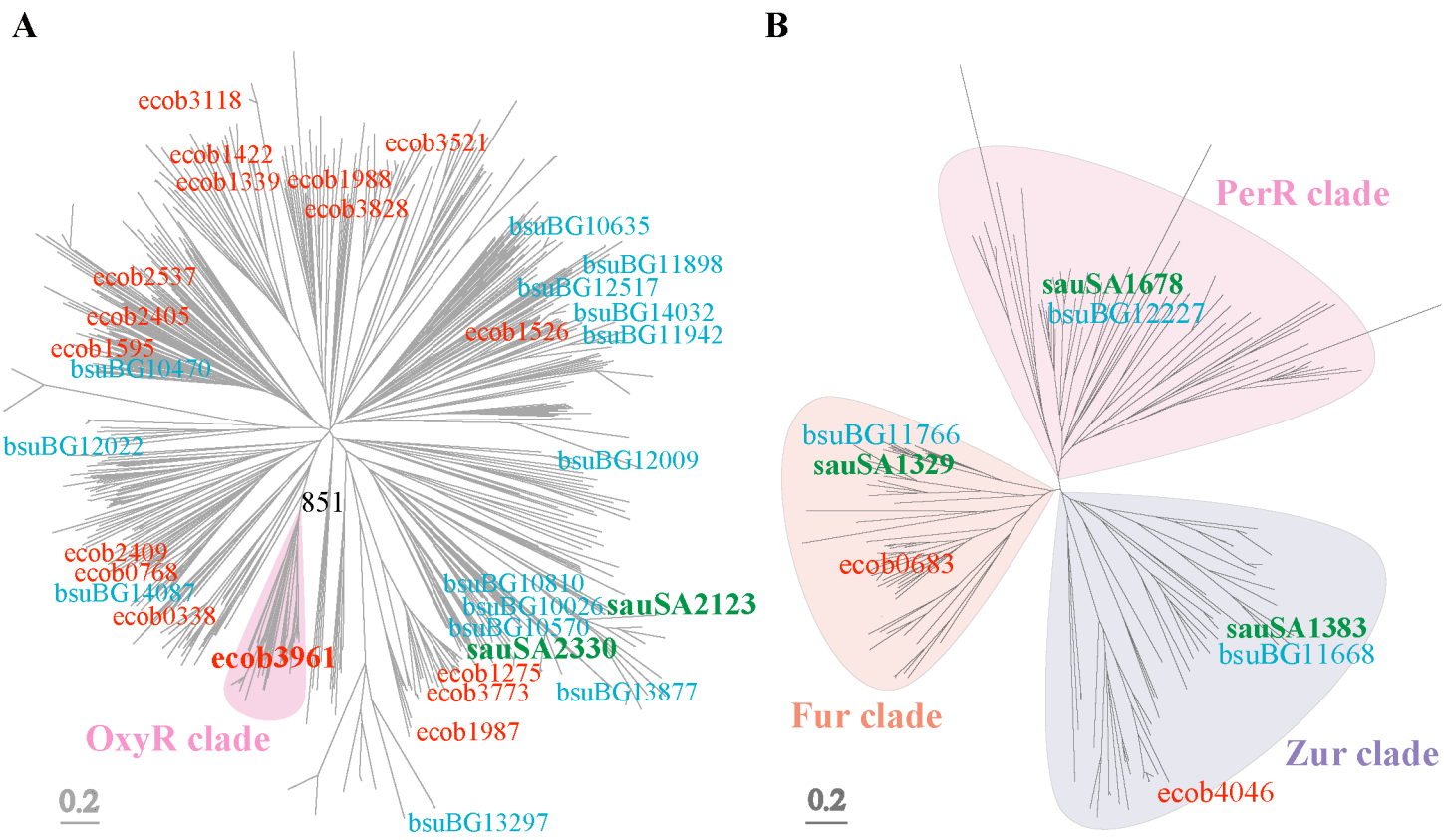
A
ecob3118
ecob1422
ecob3521
ecob1339
ecob1988
ecob3828
bsuBG10635
bsuBG11898
ecob2537
bsuBG12517
ecob2405
bsuBG14032
ecob1595
ecob1526
bsuBG11942
bsuBG10470
bsuBG12022
bsuBG12009
851
ecob2409
ecob0768
bsuBG14087
ecob0338
bsuBG10810
bsuBG10026
sauSA2123
bsuBG10570
ecob3961
sauSA2330
ecob1275
ecob3773
bsuBG13877
OxyR clade
ecob1987
0.2
bsuBG13297
B
PerR clade
sauSA1678
bsuBG12227
bsuBG11766
sauSA1329
ecob0683
sauSA1383
bsuBG11668
Fur clade
Zur clade
ecob4046
0.2

Figure 7

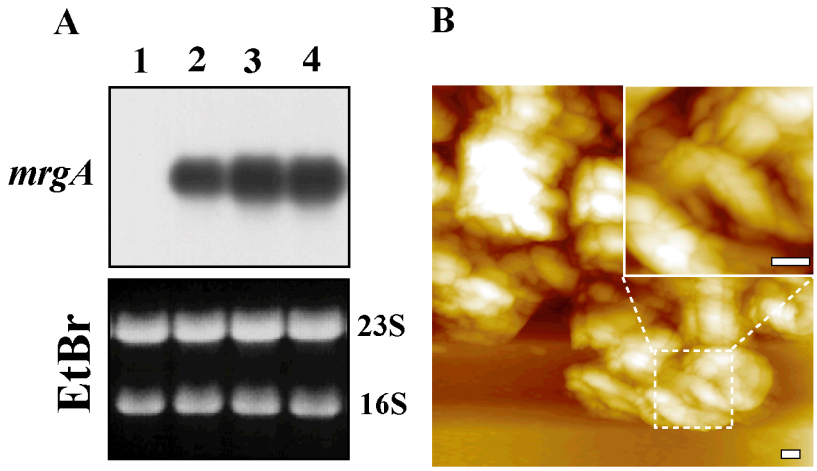

Figure 8

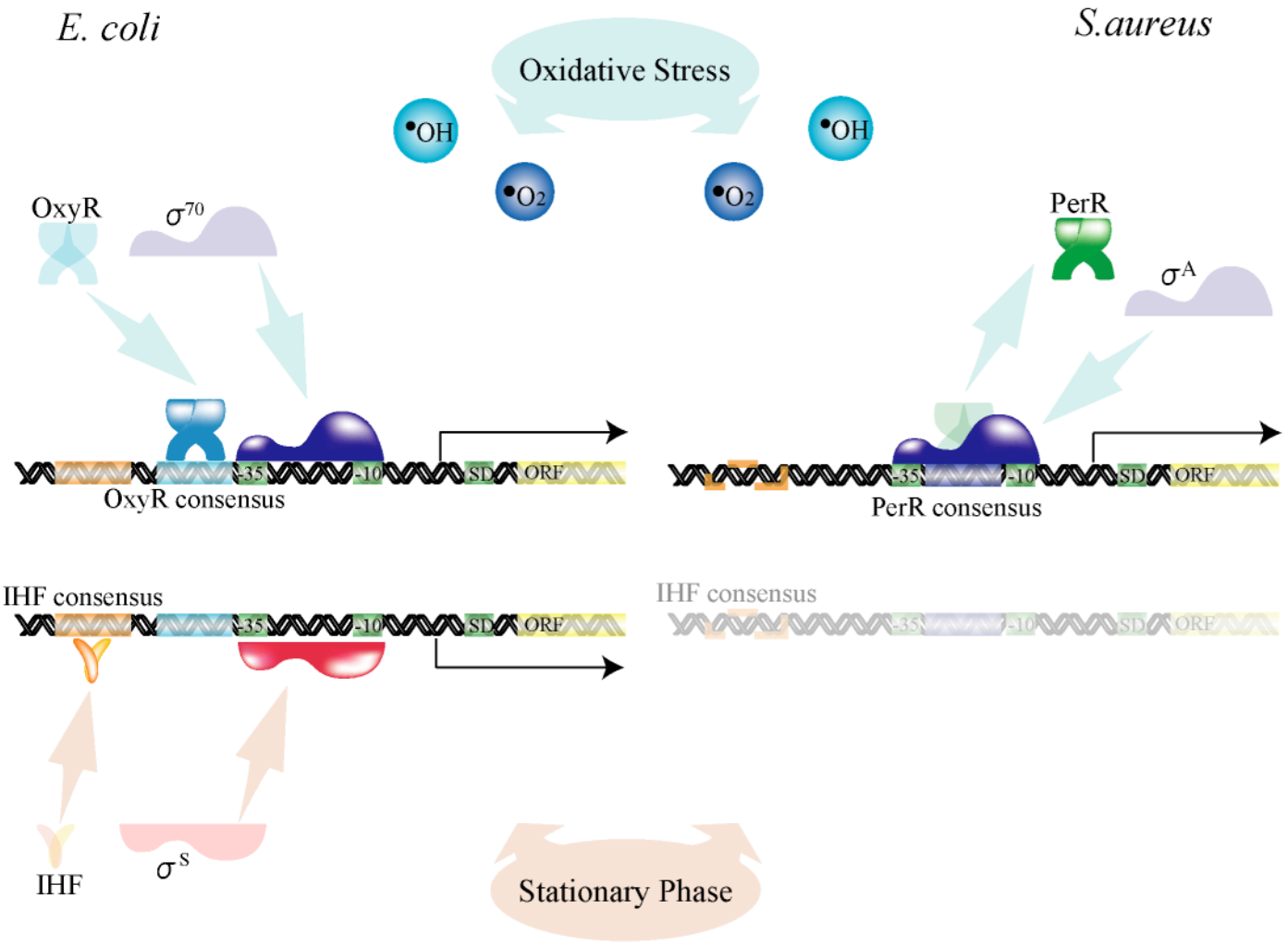
E. coli
S.aureus
Oxidative Stress
•OH
•OH
•O2
•O2
OxyR
σ70
PerR
σA
-35
-10
SD
ORF
OxyR consensus
PerR consensus
IHF consensus
IHF consensus
IHF
σS
Stationary Phase